

Strong interface localization of phonons in nonabrupt InN/GaN superlattices

E. F. Bezerra, A. G. Souza Filho, V. N. Freire, J. Mendes Filho, and V. Lemos*

Departamento de Física, Universidade Federal do Ceará, Centro de Ciências, Caixa Postal 6030, Campus do Pici, 60455-760 Fortaleza, Ceará, Brazil

(Received 3 April 2001; published 19 October 2001)

The Raman spectra of zinc-blende InN/GaN superlattices were calculated assuming the existence of an interface region with thickness δ varying from one to three monolayers. The acoustic branches are weakly affected by interfacing, but the optical branches can present frequency shifts up to 60 cm^{-1} . A downward shift is observed for the higher frequency and an upward shift for the lower frequency modes. As a consequence, the Raman peaks collapse together in the middle frequency range giving rise to a most prominent structure in the spectrum, for $\delta=3$. These effects are tracked to the localization of atomic displacements at the direct and inverse interface regions. The localization effects are strong in the InN/GaN superlattices because of the wide gap observed in the phonon density of states for both constituent materials.

DOI: 10.1103/PhysRevB.64.201306

PACS number(s): 63.20.Dj, 63.20.Pw, 68.90.+g

I. INTRODUCTION

Group III nitride semiconductors have led to high efficient quantum well (QW) structure light emitting diodes (LED's) and laser diodes (LD's) operating in the blue-green or violet region.¹ The optical and electrical processes in GaN, AlN, and InN based QW and superlattice (SL) structures are remarkably influenced by the existence of an interface. In GaAs/AlAs QW's, surface segregation leads to the generation of an atomic-scale disorder in the first overgrowth monolayers.^{2,3} Surface segregation energies in wide band-gap nitride alloys were recently calculated by Boguslawski *et al.*⁴ The authors found the segregation energies in nitrides to be one order of magnitude larger than in the arsenides or Si/Ge systems, for cation-terminated reconstructions. In addition, the nitrides differ from those systems in two distinct aspects: (i) the chemical bonds in the nitrides are significantly more ionic in character; (ii) the mismatch between the atomic radii of cations and anions is much larger in the nitrides. The latter aspect is of interest due to the increased disorder to result in wider interfaces. Actually, the indium concentration gradient across the GaN/In_{0.43}Ga_{0.57}N/Al_{0.1}Ga_{0.9}N interfaces was measured using high-resolution transmission electron microscopy (HRTEM).⁵ The HRTEM results point to a typical interface width of 1 nm for the GaN/InGaN interface while more than twice this value for the InGaN/AlGaN interface. Several studies in GaAs/AlAs SL's suggest the need to consider interface effects in describing the optical phonon spectrum.^{6,7} In the case of GaN/Al_xGa_{1-x}N SL's, Raman scattering measurements provide evidence of the graded alloy interface region to be of the order of 2 nm.⁸ This value is much larger than the interface widths found for the arsenide based SL's. However, early theoretical works on phonons in III-nitrides superlattices have disregarded interface effects. Therefore, a model to describe the lattice dynamics in the nitride based systems should include interface effects in the nanometer scale. Lattice dynamic calculations are available for GaN, AlN, and InN crystallized in the wurtzite and zinc-blende structures.^{9,10} Those calculations result in bulk-phonon frequencies to be of use in the simulation of the Raman scatter-

ing. Previous theoretical results show that interfacing effects are responsible for the lifting of degeneracies and considerable gain in intensity of Raman modes in zinc-blende GaN/AlGaN SL's.¹¹ Such effects should appear much more clearly in the InN/GaN SL's due to the greater separation of the bulk dispersion curves of their components.^{10,12}

A study of interfacing effects on the dispersion relations and Raman spectra of zinc-blende (InN)_{8- δ} /(InN_{0.5}GaN_{0.5}) _{δ} /(GaN)_{8- δ} /(InN_{0.5}GaN_{0.5}) _{δ} SL's is performed in this work, with interface thickness δ varying from one to three monolayers (ML's). The folded acoustic phonons are shown to be negligibly affected, while the confined optical mode frequencies are significantly shifted by the existence of interface. Due to the fact that the bulk dispersion relations for optical modes of InN do not overlap with those for GaN, and the acoustic phonon curves occur in a frequency range far below, the SL optical modes are either confined in one or the other layer in the ideal SL. The existence of nonabrupt interfaces strongly affects the dispersion curves with frequency shifts up to $\sim 60 \text{ cm}^{-1}$. An enhancement in the intensity of some of the Raman lines is shown to occur on increasing the interface width. The most affected mode (number 23) is an InN confined phonon that turns out to be localized in a region of about 2 ML's across the inverse InN/GaN interface for $\delta=1$. The localization of this mode is observed to occur at the direct GaN/InN interface for $\delta=2$. For $\delta=3$ the localization occurs at the inverse interface as for $\delta=1$. This mode greatly contributes to the Raman scattering in the range of frequencies between those of bulk InN and GaN. Several modes, with similar behavior, also contribute to the Raman intensity. Therefore, the Raman scattering of the GaN/InN SL's is interpreted here in terms of atomic displacement localization restricted to either the InN/GaN or the GaN/InN nonabrupt interface.

II. RESULTS AND DISCUSSION

The GaN LO mode occurs at the frequency $\omega = 740 \text{ cm}^{-1}$,¹³ while the InN LO mode occurs at $\omega = 588 \text{ cm}^{-1}$.¹⁴ The bulk selection rules forbid TO modes in a backscattering geometry of a (001) face in a crystal with

TABLE I. Bulk GaN and InN mode frequencies as used in the model to derive the force constants k , q_1 , and q_2 . The frequency values are in units of cm^{-1} .

| | LA (X) | LO (Γ) | LO (X) | k | q_1 | q_2 |
|-----|------------------|------------------|------------------|--------|-------|-------|
| GaN | 351 ^a | 740 ^b | 710 ^a | 189.71 | 32.76 | 10.00 |
| InN | 231 ^c | 588 ^d | 567 ^c | 128.20 | 26.93 | 2.77 |

^aFrom Ref. 16.

^bFrom Ref. 13.

^cFrom Ref. 10.

^dFrom Ref. 14.

either a zinc-blende or a diamond structure. By fixing this geometry, only the LO modes should play a role in the Raman scattering of a perfect superlattice constructed with those components. We first consider the ideal $\text{InN}_{n_1}/\text{GaN}_{n_2}$ superlattice, where n_i stands for the number of monolayers in each semiconductor type. The dispersion branches amounts to $N=n_1+n_2$ acoustic and N optical branches.⁷ By assuming $n_1=n_2=8$ there is a total of 32 phonon branches.

To calculate the dispersion curves, a linear chain model was employed with a plane of atoms in the actual SL represented by an atom in the linear chain.¹¹ This representation allows the associated phonons propagating along the [001] axis to be described through a one-dimensional set of equations of motion. By considering just the nearest and next-nearest-neighbor force constants, the equation of motion was solved in the harmonic approximation. The alloying at the nonabrupt interfaces was considered in the virtual-crystal approximation, which is appropriate to describe one-mode-type behavior. The interface was simulated with both constituents in equal proportion and its width was varied in steps of one monolayer up to $\delta=3$. The bond-polarizability model,¹⁵ which provides a good description of optical modes, was used to calculate the Raman spectra of the SL's. The polarizability constants were assumed to have fixed values throughout the SL. The bulk GaN and InN mode frequencies (as used in the linear chain model) and the force constants are listed in Table I. The GaN zone-center LO frequency was taken as the average value 740 cm^{-1} from experimental data of Ref. 13. The acoustic LA frequency was taken as the theoretical value of Karch *et al.*¹⁶ The InN LO(Γ) frequency was taken as the value measured by Raman scattering,¹⁴ while the zone edge phonon frequencies for this crystal were obtained from calculations.¹⁰ This kind of approach has been successfully used before to describe the optical phonon behavior in Ge/Si based superlattices.¹⁸

Calculated Raman spectra for zinc-blende $(\text{InN})_{8-\delta}/(\text{InN}_{0.5}\text{GaN}_{0.5})_{\delta}/(\text{GaN})_{8-\delta}/(\text{InN}_{0.5}\text{GaN}_{0.5})_{\delta}$ SL's are presented in Fig. 1 for several values of interface width δ . The lowest curve, for $\delta=0$, shows two dominant peaks at $\omega = 587.4 \text{ cm}^{-1}$ (mode 23) and $\omega = 739.2 \text{ cm}^{-1}$ (mode 32). These frequencies are almost coincident with the LO bulk values of InN and GaN, respectively. In between, two weak structures appear at $\sim\omega = 622 \text{ cm}^{-1}$ and $\sim\omega = 688 \text{ cm}^{-1}$, corresponding to modes 24 and 25, respectively. This identification was made by comparing the Raman frequencies with the values found in the calculated dispersion relations. To

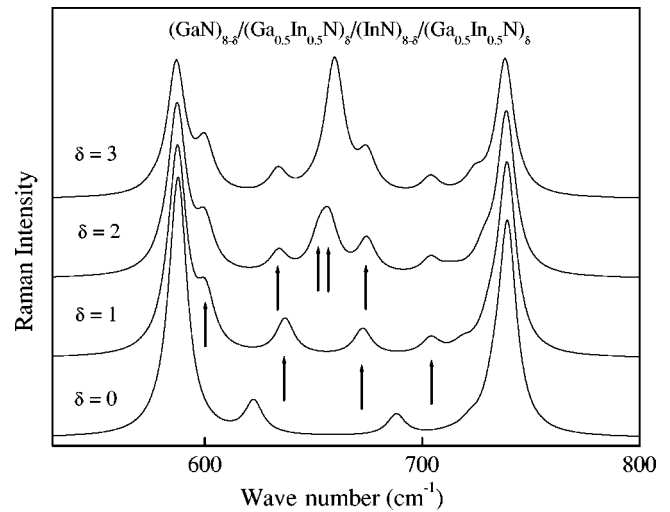


FIG. 1. Calculated Raman spectra for zinc-blende $(\text{InN})_{8-\delta}/(\text{InN}_{0.5}\text{GaN}_{0.5})_{\delta}/(\text{GaN})_{8-\delta}/(\text{InN}_{0.5}\text{GaN}_{0.5})_{\delta}$ SL's.

check for the consistency of our results a mapping was performed using the effective wave vector $q = m\pi/(n_1 + \lambda)a$, where m is the order index, a is the GaN monolayer thickness, and λ is the parameter describing the penetration of the wave function of GaN vibrations into the InN layers. The value $\lambda = 1$ was found to produce an almost perfect mapping (not shown here).

The introduction of an interface with $\delta=1$ results in a modified spectrum with the number of peaks increased in the middle range of frequency [600,710] cm^{-1} . This is shown in Fig. 1 ($\delta=1$), where the arrows indicate modes 23 to 26. A larger interface, of two monolayers, causes further increase of the number of peaks in the middle frequency range, as seen in the spectrum labeled $\delta=2$ in Fig. 1. The same set of peaks as before, is indicated by arrows in this curve. It can be noticed that the lower frequency peaks shift upward while those of higher frequency shift downward, resulting in a more crowded middle range than in the case of $\delta=1$. Figure 1 also shows a remarkable increase of the Raman intensity, particularly in the spectrum for $\delta=3$. In consequence, some of the new peaks are of the same magnitude as the original end frequency modes. For $\delta=3$ the end peaks were identified as corresponding to the modes 20 and 32, in the base of

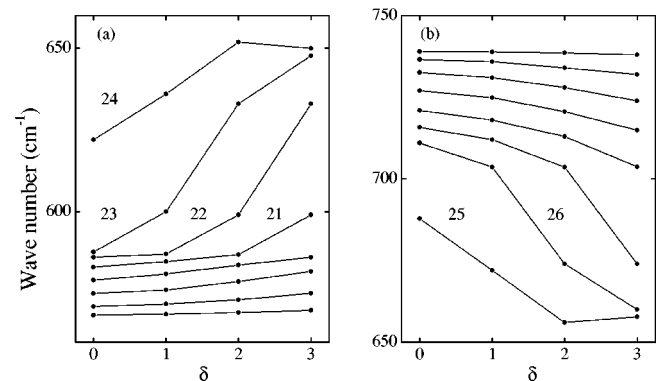


FIG. 2. Frequency versus interface thickness for the $(\text{InN})_{8-\delta}/(\text{InN}_{0.5}\text{GaN}_{0.5})_{\delta}/(\text{GaN})_{8-\delta}/(\text{InN}_{0.5}\text{GaN}_{0.5})_{\delta}$ SL.

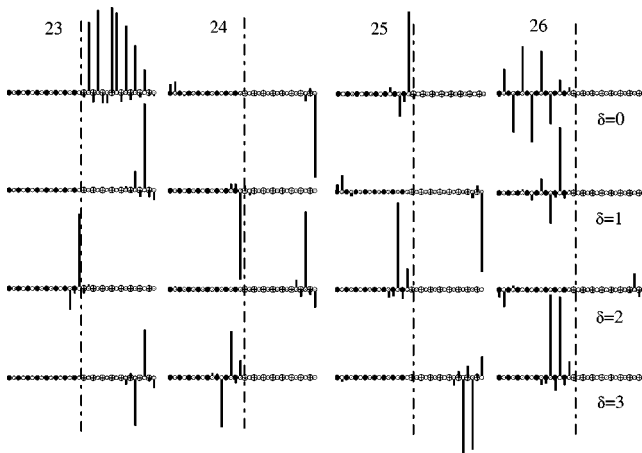


FIG. 3. Atomic displacements of selected optical modes for the $(\text{InN})_{8-\delta}/(\text{In}_{0.5}\text{Ga}_{0.5})_{\delta}/(\text{GaN})_{8-\delta}/(\text{In}_{0.5}\text{Ga}_{0.5})_{\delta}$ SL with $\delta = 0, 1, 2,$ and 3 . Open circles represent N and full circles represent Ga atoms. In atoms are represented by the biggest circles.

comparison of their frequencies with the results of the dispersion relation. It would be rushing to associate the middle range features to isolated modes, but contribution of modes 21 to 31 is expected in this range. Several dispersion curves around 588 cm^{-1} correspond to different modes for certain δ values. It occurs also around 600 cm^{-1} and 634 cm^{-1} , making it difficult for distinguishing the exact correspondence of frequency at larger interfaces with the parent $\delta = 0$ line in these dispersion relations. Due to this difficulty we analyze instead the frequency versus δ behavior. The ω vs δ plots are given in Figs. 2(a) and 2(b) for the optical modes of the SL with interfaces $\delta = 0, 1, 2$ and 3 . This figure shows that the frequency increases linearly with δ for the modes 17 to 20. For the modes 21 to 27 the ω vs δ behavior is quite anomalous. For the remaining modes, 28 to 32, the ω vs δ curves are almost linear. The anomalies can be related to localization of the vibrations at the interfaces. To test this idea, we calculated the atomic displacements in the superlattice. We found most of the modes to be confined either in the InN layer or in the GaN layer for $\delta = 0$. Modes 24 and 25 are exceptions. We observed the mode 24 to be extremely localized at the InN/GaN interface and the mode 25 at the GaN/InN interface, for $\delta = 0$. The localization is probably responsible for the existence of these modes in the Raman spectrum even for $\delta = 0$. It is worth mentioning that a previous calculation of the projected density of states for acoustic vibrations using the linear chain model shows a remarkable increase for the strongest localized modes leading to enhanced intensities.¹⁷

Figure 3 shows the atomic displacements for modes 23 to 26, and all values of interface probed in this work. It is seen in this figure that the atomic displacements change localiza-

tion of the modes 24 and 25 for $\delta = 1$ to the opposite interfaces. For $\delta = 2$ the localization pattern is similar to that observed for $\delta = 0$, and the pattern for $\delta = 3$ to that for $\delta = 1$. Figure 3 also shows that the confined mode 23 (26) in a InN (GaN) layer transforms to an interface localized mode. Both modes 23 and 26 share the property of inverting the interface localization upon changing the interface width in steps of one monolayer. The modes 17 to 20 are confined in the InN layer for all δ values. The mode 21 transforms to a highly localized mode in the center of the InN layer, for $\delta = 3$. The mode 22 is localized close to the GaN/InN interface for $\delta = 2$ and at the InN/GaN interface for $\delta = 3$. Mode 27 changes from a GaN confined mode to a localized mode across the GaN/InN interface. Finally, the GaN confined mode 28 changes to a mode localized at the center of the GaN layer, for $\delta = 3$. The four remaining modes, number 29, 30, 31, and 32 are GaN confined for any δ value.

III. CONCLUSION

Summarizing, the interface effects on the Raman spectra of zinc-blende $(\text{InN})_{8-\delta}/(\text{In}_{0.5}\text{Ga}_{0.5})_{\delta}/(\text{GaN})_{8-\delta}/(\text{In}_{0.5}\text{Ga}_{0.5})_{\delta}$ superlattices were studied using a linear chain description and the bond-polarizability model. It is shown that the optical modes region of the spectrum is severely affected by the existence of the interface regions. The main influence is the increase of intensity of peaks positioned in between those related to the end spectra InN-confined and the GaN-confined modes. These peaks were seen to shift with increasing δ towards the center position in the spectrum. The $\delta = 3$ interface effects in the Raman intensities are drastic, giving rise to a most prominent structure in the middle frequency range of the spectrum. This structure results from the overlap of several modes in a short frequency range. Examination of atomic displacements allowed for the effects to be tracked to localization of the vibrations. These effects are much stronger than those observed previously for other systems like GaAs/AlAs, Si/Ge, and AlN/GaN SL's. The results suggests that optical modes are well suited as probe for interfacing with both frequency and intensity, highly affected. The results are particularly attractive in order to compare with experiments when the samples become available.

ACKNOWLEDGMENTS

The authors acknowledge Dr. M. A. Araújo Silva for the permission to use the computer code used in the calculations. The authors would like to acknowledge the Conselho Nacional de Desenvolvimento Científico e Tecnológico (CNPq), and Fundação de Amparo à Pesquisa do Estado do Ceará (FUNCAP), for financial support.

*Author to whom correspondence should be addressed. Email: volia@fisica.ufc.br

¹S. Nakamura, *Semicond. Sci. Technol.* **14**, R27 (1999); S. Nakamura, *The Blue Laser Diode—GaN Based Light Emitters and Lasers* (Springer, Berlin, 1997).

²K. Leosson, J.R. Jensen, W. Langbein, and J.M. Hvam, *Phys. Rev. B* **61**, 10 322 (2000).

³V. Lemos, C.S. Sérgio, A.P. Lima, A.A. Quivy, R. Enderlein, J.R. Leite, and W. Carvalho, Jr., *Radiat. Eff. Defects Solids* **146**, 187 (1998), and references therein.

- ⁴P. Boguslawski, K. Rapawicz, and J.J. Bernholc, *Phys. Rev. B* **61**, 10 820 (2000).
- ⁵C. Kisielowski, Z. Liliental-Weber, and S. Nakamura, *Jpn. J. Appl. Phys., Part 1* **36**, 6932 (1997).
- ⁶K.T. Tsen, *J. Raman Spectrosc.* **27**, 277 (1996); K.T. Tsen, D.J. Smith, S.C.Y. Tsen, N.S. Kumar, and H. Morkoç, *J. Appl. Phys.* **70**, 418 (1991).
- ⁷B. Samson, T. Dumelow, A.A. Hamilton, T.J. Parker, S.R.P. Smith, D.R. Tilley, C.T. Foxon, D. Hilton, and K.J. Moore, *Phys. Rev. B* **46**, 2375 (1992).
- ⁸D. Behr, R. Niebuhr, J. Wagner, K.-H. Bachem, and U. Kaufmann, *Appl. Phys. Lett.* **70**, 363 (1997).
- ⁹G. Kaczmarczyk, A. Kaschner, S. Reich, A. Hoffmann, C. Thomsen, D.J. As, A.P. Lima, D. Schikora, K. Lischka, R. Averbeck, and H. Riechert, *Appl. Phys. Lett.* **76**, 2122 (2000).
- ¹⁰F. Bechstedt, U. Grossner, and J. Furthmüller, *Phys. Rev. B* **62**, 8003 (2000).
- ¹¹E.F. Bezerra, V.N. Freire, A.M.R. Teixeira, M.A. Araújo Silva, P.T.C. Freire, J. Mendes Filho, and V. Lemos, *Phys. Rev. B* **61**, 13 060 (2000).
- ¹²C. Bungaro, K. Rapcewicz, and J. Bernholc, *Phys. Rev. B* **61**, 6720 (2000).
- ¹³H. Siegle, L. Eckey, A. Hoffmann, C. Thonsen, B. Meyer, D. Schikora, H. Hanken, and K. Lischka, *Solid State Commun.* **96**, 943 (1995); M. Giehler, M. Ramstainer, O. Brandt, H. Yang, and K.H. Ploog, *Appl. Phys. Lett.* **67**, 733 (1995); A. Tabata, A.P. Lima, J.R. Leite, V. Lemos, D. Schikora, B. Schöttker, U. Köhler, D. As, and K. Lischka, *Semicond. Sci. Technol.* **14**, 318 (1999).
- ¹⁴A. Tabata, A.P. Lima, L.K. Teles, L.M.R. Scolfaro, J.R. Leite, V. Lemos, B. Schöttker, T. Frey, D. Schikora, and K. Lischka, *Appl. Phys. Lett.* **74**, 362 (1999); A. Tabata, J.R. Leite, A.P. Lima, E. Silveira, V. Lemos, T. Frey, B. Schöttker, D. Schikora, and K. Lischka, *Appl. Phys. Lett.* **75**, 1095 (1999).
- ¹⁵B. Jusserand and M. Cardona, in *Light Scattering in Solids V*, edited by M. Cardona and G. Güntherodt, *Topics in Applied Physics*, Vol. 66, p. 49 (Springer, Heidelberg, 1989).
- ¹⁶K. Karch, J.-M. Wagner, and F. Bechstedt, *Phys. Rev. B* **57**, 7043 (1998).
- ¹⁷M.A.A. Silva, E. Ribeiro, P.A. Schulz, F. Cerdeira, and J.C. Bean, *Phys. Rev. B* **53**, 15 871 (1996); *J. Raman Spectrosc.* **27**, 257 (1996).
- ¹⁸V. Lemos, O. Pilla, and M. Montagna, *J. Braz. Chem. Soc.* **7**, 471 (1996).